HHS Public Access

Author manuscript

Food Chem Toxicol. Author manuscript; available in PMC 2021 May 01.

Published in final edited form as:

Food Chem Toxicol. 2020 May ; 139: 111186. doi:10.1016/j.fct.2020.111186.

Comparison of Liver Regeneration after Partial Hepatectomy and Acetaminophen-induced Acute Liver Failure: A Global Picture Based on Transcriptome Analysis

Bharat Bhushan[1], **Sumedha Gunewardena**[2], **Genea Edwards**[3], **Udayan Apte**[3]

[1]Department of Pathology, School of Medicine, University of Pittsburgh, Pittsburgh, PA

[2]Department of Molecular and Integrative Physiology, University of Kansas Medical Center, Kansas City, KS

[3]Department of Pharmacology, Toxicology and Therapeutics, University of Kansas Medical Center, Kansas City, KS

Abstract

Liver regenerates following surgical removal and after drug-induced liver injury (DILI). However, most of the mechanisms of liver regeneration were identified using partial hepatectomy (PHX) model rather than using DILI models. We compared mechanisms of liver regeneration following PHX and after acetaminophen (APAP) overdose, a DILI model, using transcriptomic approach. Kinetics of hepatocyte proliferation and global gene expression profiles were studied in male C57BL/6J mice either subjected to PHX or following APAP overdose. Liver regeneration was much more synchronized after PHX as compared to APAP overdose. Transcriptomics analysis revealed activation of common upstream regulators in both models including growth factors HGF, EGF and VEGF; and cytokines IL6 and TNFα. However, magnitude of activation and temporality was significantly differed between the two models. HGF and VEGF showed similar activation between PHX and APAP but activation of EGF was significantly stronger in the APAP model. Activation of IL6 and TNFα transcriptional programs was delayed but remarkably higher in APAP. These dissimilarities could be attributed to inherent differences in the two models including significant injury and inflammation exclusively in the APAP model. This study highlights need to study mechanisms of liver regeneration after DILI separately from the mechanisms of regeneration PHX.

Introduction

Liver regeneration is one of the most fascinating characteristics of the liver, which plays a critical role in liver homeostasis (1–4). Whereas ability of liver to regenerate has been known for centuries, systematic studies on the mechanisms of liver regeneration have been conducted since the 1930s after Anderson and Higgins revealed the rodent partial hepatectomy (PHX) model (5). Since then, extensive mechanistic information about signals involved in initiation and more recently, in termination of liver regeneration have been

Corresponding Author: Udayan Apte, PhD, DABT, Department of Pharmacology, Toxicology and Therapeutics, University of Kansas Medical Center, 3901 Rainbow Blvd, MS1018, Kansas City, KS 66160, Tel: (913) 588-9247, uapte@kumc.edu.

obtained (3, 6–9). Most of these data were generated using the PHX model in rodents, where 2/3rd of the liver is surgically removed and the remnant liver is allowed to grow back. PHX has clinical significance because many patients undergo partial liver resection for a variety of hepatic diseases (10). Additionally, with the advent of living donor liver transplantation, liver regeneration after PHX has gained new significance (11). Liver also regenerates following drug-induced liver injury (DILI) and plays a critical role in prevention of acute liver failure (ALF) following DILI (12, 13). Liver regeneration after DILI has been demonstrated using model hepatotoxicants, environmental contaminants that target the liver, and following overdose of drugs such as acetaminophen, the most popular anti-pyretic and analgesic agent (12, 14–20). It is known that liver regeneration is a critical determinant of final outcome of ALF following APAP overdose and patients with better innate liver regeneration have better spontaneous transplant free survival (17, 21–24). Thus, regenerative therapies hold great therapeutic potential for APAP-induced ALF and DILI in general. However, the mechanisms of liver regeneration following DILI are not as well studied as the mechanisms of liver regeneration after PHX. This is mainly because of the assumption that factors involved in regeneration are similar in liver regeneration after PHX and that after DILI. However, a systematic comparison of mechanisms of liver regeneration after PHX and after DILI is lacking.

In this study, we have compared kinetics of hepatocyte proliferation and changes in transcriptomic profile during liver regeneration following PHX and liver regeneration following APAP-induced ALF in mice, the most common cause of DILI in the Western world (25–27). Analyzing transcriptional networks based on global gene expression profile, this study directly compares and provides insight on the mechanisms of liver regeneration following PHX and after APAP-induced liver injury in mice, which will be foundational for more targeted studies in the future.

Methods

Animals, Surgeries, Treatments and Tissue Harvesting

Two to three month old male C57BL/6J mice purchased from the Jackson Laboratories (Bar Harbor, ME) were used in these studies. All animals were housed in Association for Assessment and Accreditation of Laboratory Animal Care-accredited facilities at the University of Kansas Medical Center under a standard 12-hr light/dark cycle with access to chow and water *ad libitum* (unless specified). The Institutional Animal Care and Use Committee at University of Kansas Medical Center approved all studies. PHX surgeries were performed as previously described (28). For APAP overdose studies, mice were treated (ip) with 300 mg/kg APAP (dissolved in warm saline) after overnight fasting as described before (21). Mice were sacrificed at 0, 3, 6, 12, 24 and 48 hr time points for both studies; livers were collected as described before (28). Liver samples were processed to obtain paraffin sections and RNA samples as described before (28).

Microarray Analysis

Microarray analysis was performed on pooled RNAs isolated from liver samples at each time points (0, 3, 12, 24 and 48 hr) from APAP and PHX groups using the GeneChip®

Mouse Genome 430 2.0 Array Set 430 (Affymetrix, Santa Clara, CA). Significantly expressed genes were analyzed using Ingenuity Pathways Analysis (IPA, Ingenuity Systems, version 01–10). For temporal analysis, set of genes upregulated or downregulated (2-fold cutoff) at various time points in both groups (APAP and PHX) with respect to corresponding basal levels, along with the respective fold change values were uploaded to the IPA software tool. For inter-group analysis, set of genes upregulated or downregulated (2-fold cutoff) in the APAP group compared to the PHX group at each time point, along with the respective fold change values were uploaded to the IPA software tool. Activation or inhibition of the upstream regulators was predicted based on changes in the downstream gene expression patterns.

H&E Staining and PCNA Immunohistochemistry

Paraffin-embedded liver sections (4 μm thick) were used for H&E staining and immunohistochemical detection of PCNA as described before (21, 28).

Statistical Analysis

Data presented in the form of bar graphs show mean ± SEM. Statistically significant difference was determined between two groups using paired Student's T-test and for more than two groups by using ANOVA. Difference between the groups was considered statistically significant at $P<0.05$.

Results

Extensive hepatocyte injury and dispersed proliferative response after APAP overdose as compared to PHX

Histopathological analysis of H&E stained liver section indicated extensive liver injury only in the livers of APAP treated mice with no detectable cell death in livers after PHX (Fig. 1A (a-j)). This was further confirmed by quantification of necrotic areas in both models (Fig. 1B). Overt hepatic necrosis after APAP overdose was first visible at 6 hr after APAP treatment and peaked at 12 hr. However, absolutely no necrosis was observed in the regenerating lobes after PHX. Proliferating cell nuclear antigen (PCNA) staining revealed temporally dispersed proliferative response after APAP overdose. Rapid and earlier increase in cell proliferation was observed after APAP overdose (Fig 1A (k-t) and Fig. 1C). PCNA positive cells could be detected in the livers of APAP treated mice as early as 3 hr after APAP treatment, which increased by 12 hr and remained substantially elevated for the remaining time course (up to 48 hr) after APAP treatment (Fig. 1A (p-t)). In contrast, proliferative response was more synchronized after PHX and extensive proliferation was observed only at 48 hr after PHX (Fig.1A (k-o)). However, the peak of proliferation was comparable and was attained at similar time point (48 hr) in both APAP and PHX models (Fig. 1C). PCNA data was also supported by mRNA expression of Cyclin D1 which is a critical mediator that governs entry into the cell cycle. Early (at 3 hr) small but significant induction of Cyclin D1 (~2 fold increase) was observed exclusively after APAP treatment (Fig. 9A). However, major peak of induction (~7 fold increase in both models) was observed at similar time point (12 hr) in both models (Fig. 9A). Whereas, cell proliferation was

observed in the areas surrounding necrotic areas in the livers of APAP treated mice, it was observed over the entire lobule in the PHX samples.

Comparative analysis of upstream regulators predicted to be altered after APAP overdose and PHX

Next, microarray analysis was performed on the samples from APAP and PHX groups at various time points (0, 3, 12, 24 and 48 hr). Fold change in gene expression was calculated for each group and each time point by comparing to their respective 0 hr control groups and resulting data were analyzed using Ingenuity Pathway Analysis (IPA) to look at a global picture of the gene expression profile. Alteration of upstream regulators after APAP overdose or PHX was predicted based on the global expression profile of downstream genes keeping both the directionality and intensity of changes in gene expression into consideration. Heat-map showing comparison of top 30 upstream regulators predicted to be alerted at various time points after APAP overdose or PHX compared to corresponding basal levels is presented in Fig. 2A. Overall, there were striking similarities in altered upstream regulator profile between the APAP and PHX models, with several key regulators of liver regeneration among top upstream regulators activated in both models (Fig. 2A). These included growth factors such as HGF, EGF and PDGF; cytokine mediators such as IL6/STAT3 and TNF/NFκB; angiogenic factors such as VEGF; MAPKs such as ERK and p38; and anti-mitogenic mediators such as TGFβ1 (Fig. 2A). In spite of these similarities, there were temporal differences in activation of some of the regulators including IL6 (Fig. 2A). Further, overall activation of several of the upstream regulators was higher in APAP model compared to the PHX model resulting in significant differences in activation of these regulators upon direct comparison between APAP and PHX at a particular time point (Fig. 2A and B).

Heat-map showing direct comparison of top 30 upstream regulators predicted to be significantly alerted in APAP vs PHX model at various time points is presented in Fig. 2B. Of note, activation of cytokines such as TNF and IL1β, growth factors such as EGF and PDGF, and TGFβ1 was significantly higher in the APAP model compared to the PHX model (Fig. 2B). These differences were especially striking at 12 and 24 hr time points, which might be related to extensive liver injury and inflammation exclusively observed in the APAP model. These analyses are further comprehensively described in the following sections.

Similarities in the signaling pathways predicted to be altered after APAP overdose and PHX

A number of cytokines, chemokines and growth factors have been implicated in liver regeneration (29). Hepatocyte growth factor (HGF) is the ligand for receptor cMET and is considered critical for hepatocyte proliferation and liver regeneration after PHX (8). Dose-dependent c-MET activation has also previously reported in the APAP model, but its role in liver regeneration after APAP overdose has not directly investigated (17). Peak activation of HGF downstream gene network was observed at 48 hr, the time point of peak proliferation after both APAP overdose and PHX (Fig. 2A and Fig. 3). Although activation of HGF gene signature appear to be higher in PHX compared to APAP at 48 hr (z-score for HGF

activation was 4.926 and 6.337 in APAP and PHX group, respectively), numerous HGF downstream genes were induced in both APAP and PHX groups compared to basal levels (Fig. 2A and Fig. 3). High order of p-value (1.26×10^{-32} and 1.72×10^{-31} for APAP and PHX, respectively) of overlap between HGF downstream genes induced in both the experimental groups vs. HGF downstream genes in the reference genome demonstrate robust alteration of HGF network in both APAP and PHX models. This is further supported by previous reports demonstrating remarkable phosphorylation (i.e. activation) of MET after both APAP and PHX in mice (17, 30).

Angiogenesis and restoration of microvasculature is also an important aspect of liver regeneration after both acute liver injury and surgical resection. VEGF is a mitogen for endothelial cells and is known to play an important role in angiogenesis during liver regeneration in both PHX and APAP models (8, 13). Similar to HGF, VEGF downstream gene network was strongly activated in both APAP and PHX groups compared to basal levels, with peak of activation at 48 hr (p-value: 1.03×10^{-28} and 7.88×10^{-28} for APAP and PHX groups, respectively) (Fig. 2A and Fig. 4). However, VEGF activation appeared to be slightly higher and had sharp peak (at 48 hr) in the PHX model, while it was more temporally dispersed in the APAP model (z-score for VEGF activation was 5.55 and 7.163 at 48 hr in APAP and PHX groups, respectively) (Fig. 2A and Fig. 4).

Apart from activation of several upstream regulators, a few regulators (including Let-7, ACOX1 and α-catenin) were predicted to be consistently inhibited over entire time-course in both APAP and PHX models (Fig. 2A). Temporal similarities for inhibition of miRNA Let-7 between APAP and PHX groups were especially notable. Let-7 was consistently inhibited at all the time points compared to basal levels in both the models with peak of inhibition at 48 hr (Fig. 2A). Z-scores for Let-7 inhibition and p-values of overlap with reference Let-7 network were comparable in APAP and PHX models at 48 hr (APAP: −6.433 (z-score), 2.49×10^{-26} (p-value); PHX: −5.872 (z-score), 5.09×10^{-25} (p-value)). Most of the downstream genes which are known to be inhibited by Let-7 miRNA were induced in both APAP and PHX models (Fig. 5).

Dissimilarities in the signaling pathways predicted to be altered after APAP overdose and PHX

Apart from above described similarities between the APAP and PHX models, there were differences in the time course and magnitude of activation of several upstream regulators, especially cytokines such as IL6 and TNF, which are known to optimize timely liver regeneration in both APAP and PHX models (Fig. 2A and B) (8, 13). Based on the expression profile of downstream genes, IL6 was found to be remarkably activated as early as 3 hr after PHX. IL6 activation was maintained at 12 hr and decreased at later time points after PHX (Fig. 2A). In contrast, IL6 activation was delayed in APAP model. Significant IL6 activation was observed only at 12 and 24 hr after APAP and declined sharply at 48 hr (Fig. 2A). Direct comparison of APAP and PHX groups at specific time points revealed significant inhibition of IL6 gene network in APAP vs PHX group at 3 hr (i.e. activation was more in PHX compared to APAP group at this time point) with z-score of −2.47 and p-value of 1.36×10^{-29} (Fig. 2B and 6A). However, at 24 hr, IL6 activation pattern was reversed with

significantly higher activation in APAP compared to PHX group with z-score of 4.135 and p-value of 2.49×10^{-32} (Fig. 2B and 6B). This was further corroborated by higher phosphorylation (i.e. activation) of transcription factor STAT3 in APAP group compared to PHX, which occurs downstream of IL6 signaling (Fig. 9C). Similar strikingly higher phosphorylation was also observed for JNK 1/2 in APAP model along with higher expression of downstream transcription factors c-Jun and ATF (Fig. 9D and E). Apart from its role in liver regeneration and hepatocyte proliferation, JNK signaling is also considered important for mediating APAP overdose–induced liver injury (17). Similar to IL6, TNF activation appeared to be higher in PHX compared to APAP group at 3 hr, but it was more strongly activated in APAP group at 12 and 24 hr (Fig. 2A). Direct comparison of APAP and PHX groups at specific time points revealed significant activation of TNF gene network in APAP vs PHX group at 12 and 24 hr (Fig. 2B). In fact, based on downstream gene signature, TNF was the topmost upstream regulator activated in APAP compared to PHX group at 24 hr with outstanding z-score of 7.489 and p-value of 2.16×10^{-47} (Fig. 7A). To corroborate, induction of TNF-α mRNA was also strikingly higher after APAP treatment compared to PHX (Fig. 9B).

TGFβ signaling is considered to be mito-inhibitory during liver regeneration after PHX (8). Recent studies also reported an important role of TGFβ in liver injury and impairment of liver regeneration in the APAP overdose model (31, 32). Time-course analysis of upstream regulators in comparison to the basal levels in both models as well as direct comparison of APAP vs PHX groups revealed that TGFβ activation was remarkably stronger at 12 and 24 hr in APAP compared PHX group (Fig. 2A and B). Significant activation of TGFβ gene signature at 24 hr (activation z-score: 4.087 and p-value: 8.21×10^{-29}) in APAP vs PHX group is depicted in Fig. 7B. Similar to activation of HGF, growth factors EGF and PDGF were activated after both APAP overdose and PHX, but activation was significantly stronger in APAP model, especially at 12 and 24 hr (Fig. 2A and B). In fact, direct comparison of APAP and PHX groups revealed that downstream gene network of EGF and PDGF was significantly activated in APAP as compared to PHX at 24 hr with p-value of 9.2×10^{-29} and 3.38×10^{-30}, respectively and z-score of 5.279 and 6.122, respectively (Fig. 2B and Fig. 8). Our previous study has reported strong and sustained EGFR activation after APAP overdose in mice (24). Overall, several upstream regulators were predicted to be significantly activated in APAP group compared to PHX group at peak time points of liver injury after APAP overdose (i.e. 12 and 24 hr) (Fig. 2B).

Discussion

Liver regeneration is the most striking feature of liver pathobiology and is critical for maintaining liver health (3, 4). Extensive investigations in the past few decades have revealed some of the mechanisms of liver regeneration (3, 29). The majority of this information has been obtained by using partial hepatectomy (PHX) in rodents as the experimental model. Relatively less is known about the molecular mechanisms of liver regeneration following drug-induced liver injury, where liver regeneration is the critical determinant of final outcome of drug overdose or acute toxic exposure (12, 15, 33, 34). No systematic evaluation of similarities and differences in the molecular mechanisms of liver regeneration after PHX and that after drug-induced liver injury has been performed. This is

the first such report, where the mechanisms of liver regeneration after PHX and acetaminophen (APAP)-induced liver injury, a clinically relevant model for drug-induced liver injury are compared using transcriptomics data.

Our study demonstrated that the magnitude of regenerative response was comparable after PHX and APAP (300 mg/kg) overdose. A sharp single peak of cell proliferation was observed at 48 hr after PHX, whereas cell proliferation was distributed over a time course of 12 to 48 hr after APAP overdose. Our previous study has shown that in spite of early entry of hepatocytes into cell cycle after APAP (300 mg/kg) overdose, majority of cells undergo DNA synthesis (S-phase) only at 48 hr, similar to the PHX model (17). We also observed a very small but significant increase in PCNA positive cells at very early time point (3 hr), specifically in the APAP model. The differences in kinetics of proliferation in APAP and PHX models are most likely driven by the inherent differences in these two models (Table 1). Liver regeneration after PHX has a clear starting point (the time of liver resection) resulting in a synchronized cell cycle in the remnant regenerating liver. There is very minimal liver injury and minor inflammatory cell infiltration after PHX in the regenerating lobes. In contrast, APAP induces extensive centrilobular (zone 3) necrotic cell death, which is followed by significant inflammatory response. Liver regeneration is in response to cell death, which in turn depends on the dose used. The time of initiation of regeneration and degree of regenerative response changes depending on the dose of APAP (or any other toxic chemical for that matter) used for the study (35). Additionally, in PHX model, entire remnant liver undergoes regeneration but following toxic injury mainly the cells surrounding the necrotic zone undergo proliferation. These characteristics result in an unsynchronized cell cycle during regeneration after APAP-induced liver injury.

Hepatocyte growth factor (HGF) and epidermal growth factor (EGF) and their receptors c-Met and EGFR, respectively, play a critical role in liver homeostasis and liver regeneration after PHX (30, 36). This is highlighted by the fact that only combined disruption of these signaling pathways, not any other extracellular signaling pathways, results in complete elimination of liver regeneration after PHX (30). This is also observed in a chemical mitogen–induced hepatomegaly model, which does not involve any tissue injury or tissue loss (37). Our previous study demonstrated that cMET and EGFR are activated even after APAP overdose in a dose-dependent manner (17, 24). EGFR activation was also observed in APAP-treated primary human hepatocytes in a serum free medium (24). Thus, it is not surprising that HGF and EGF were among the top activated upstream regulators in both APAP and PHX models. Activation of HGF gene signature was comparable in both APAP and PHX models with peak activation at 48 hr in both models. However, activation of EGF gene signature was significantly stronger in the APAP model, especially during the peak of liver injury. Our previous study indeed showed strong EGFR activation preceding liver injury and demonstrated its causative role in APAP hepatotoxicity in mice (24). In this study, early EGFR inhibition completely prevented APAP-induced liver injury without altering APAP metabolism (24). This study also demonstrated that liver regeneration after APAP overdose is more critically dependent on EGFR activation compared to PHX (24). In PHX model, inhibition of EGFR alone (without disrupting c-MET signaling) has been shown to have only mild effect on liver regeneration (30). However, inhibition of EGFR (after APAP toxicity was already established) almost completely abolished compensatory hepatocyte

proliferation, resulting in progression of liver injury and mortality after APAP overdose (24). These findings indicate that EGFR signaling plays a mechanistically different role in APAP-induced ALF as compared to the PHX.

Apart from growth factors, cytokines such as IL-6 and TNF-α also assist in orchestrating timely and optimal liver regeneration response after PHX (8). In contrast to growth factors described above, cytokines are neither direct mitogens for hepatocytes in culture nor they can standalone cause hepatocyte proliferation after in vivo administration (8). Further, IL-6 or TNF receptor 1 (TNF-R1) deletion in mice only delays liver regeneration after PHX, without impacting final recovery of the liver mass (9). Increased expression of IL-6 and TNF-α and activation of their downstream signaling mediators STAT3 and NF-κB also occur after APAP overdose (17). While IL-6 signaling increases in a dose-dependent manner after APAP overdose, TNF-α signaling decreases after severe APAP overdose, that causes impaired liver regeneration (17). Similar to the PHX model, both deletion of IL-6 or TNF receptor 1 (TNF-R1) in mice has been shown to lower liver regeneration after APAP overdose (38, 39). However, recovery was only slightly delayed (in IL-6 KO mice) or not affected(in TNF-R1 KO mice) indicating their role is dispensable even in the APAP model similar to PHX (38, 39). In this study, among other cytokines and chemokines, both TNF-α and IL-6 (along with their downstream signaling mediators STAT3 and NF-κB) were among the top upstream regulators activated in both APAP and PHX models. However, there were temporal differences in the activation of gene signatures of these cytokines in APAP and PHX models. While activation of these cytokines was observed very early (3 hr) in the PHX model, delayed (at 12–24 hr) but much stronger activation was observed in the APAP model. These differences are most likely related to presence of massive liver injury and inflammation in the APAP model and potential role of these cytokines in these processes. In fact, apart from altering liver regeneration, TNF-R1 KO has been shown to increase initial liver injury in the APAP model (40). These data highlight the fact that liver injury and subsequent inflammation add additional layers of complexities to the process of liver regeneration in the APAP model. In order to understand a direct role on any mediator in liver regeneration, secondary effects due to role of that mediator in liver injury must be considered.

As previously mentioned, dose dependency of regenerative response is another characteristic of the APAP model that distinguishes it from the PHX model. Our previous study has shown that moderate APAP overdose (300 mg/kg) causes robust and timely regenerative response, while severe APAP overdose (600 mg/kg) causes delayed and impaired liver regeneration resulting in failed recovery (17). Although similar failed regenerative response is also obtained after extensive hepatectomy (90%), but the underlying mechanisms of regenerative failure are different compared to the APAP model. After 90% hepatectomy, liver lacks critical mass necessary to initiate liver regeneration. However, after severe APAP overdose (600 mg/kg), lack of critical mass is not an issue as more than 50% hepatocytes are still viable even at the time points of peak liver injury (17). Further, many critical pro-regenerative pathways including growth factor signaling (via HGF/cMET and EGF/EGFR), cytokine signaling (via IL6/STAT3) and MAPKs signaling (via ERK1/2) remain highly activated even after severe APAP overdose (17). Our and other studies have demonstrated role of activation of cell cycle arrest pathways, including p53 and p21 in this impaired

regenerative response after severe APAP overdose (31, 41–43). Further, a recent study has shown a role of TGFβ signaling in increased p21 activation and spreading of hepatocellular senescence to uninjured areas (surrounding necrotic zones) after APAP overdose (31). TGFβ transcriptional signature was more strongly activated in the APAP model compared to PHX model in our comparative analysis. Thus, in contrast to the PHX model, there is signaling transduction most likely driven by injury-related stress that promote active cell cycle inhibition in uninjured hepatocytes, resulting in impaired liver regeneration after severe APAP overdose. In APAP model, apart from understanding mechanisms that promote liver regeneration, it is critical to understand mechanisms which impair liver regeneration after severe APAP overdose. This is important from clinical standpoint as treatment strategies are required specifically for patients who cannot regenerate spontaneously. Thus, based on our data and previous study demonstrating beneficial effect of pharmacological inhibition of TGF-βR1 in APAP-induced liver injury even after severe APAP overdose, targeting TGF-β signaling can be a promising therapeutic strategy for stimulating liver regeneration during APAP-induced ALF (31).

To our knowledge, this is the first comparative analysis of global transcriptional signatures to understand the mechanisms of liver regeneration after PHX and after APAP-induced liver injury. Although both models appear to have many similarities, the exact signaling events controlling cell proliferation after APAP-induced liver injury may differ substantially from the PHX model. Our global analysis will be foundational for other more targeted studies to delineate these differential mechanisms of liver regeneration in these models. Our study raises many further questions. We used APAP-induced liver injury for this study as a model because of its obvious clinical relevance. Will the mechanisms of liver regeneration be similar if a toxic chemical that acts via a different mechanism of action (for e.g. CCl_4 or thioacetamide)? Further, would the mechanisms of regeneration be different if the type of cell death induced by the toxicant is different, for examples necrosis as in the case of APAP vs apoptosis as in the case of LPS/galactosamine combination? Furthermore, will the regenerative signaling be different in cases of acute liver injury induced by viral hepatitis, a major cause of acute liver failure in developing countries, especially in Asia? Whereas these questions are currently unanswered, our study has highlighted that the mechanisms and kinetics of liver regeneration are different depending on etiology of the liver damage and a more focused model-specific analysis of mechanisms of regeneration are warranted in the future.

Financial Support:

These studies were supported by NIH - P20 RR021940, DKR0198414, and AASLD/ALF Liver Scholar Award (Udayan Apte).

Keywords:

HGF Hepatocyte growth factor

EGF epidermal growth factor

VEGF vascular endothelial growth factor

TNFα	tumor necrosis factor alpha
IL6	interleukin 6

List of Abbreviations:

APAP	acetaminophen
PHX	partial hepatectomy
ALF	acute liver failure
DILI	drug-induced liver injury
H&E	hematoxylin and eosin
PCNA	proliferating cell nuclear antigen

References

1. Diehl AM. Liver regeneration. Front Biosci 2002;7:e301–314. [PubMed: 12086922]
2. Fausto N Liver regeneration. J Hepatol 2000;32:19–31.
3. Michalopoulos GK. Liver regeneration. J Cell Physiol 2007;213:286–300. [PubMed: 17559071]
4. Michalopoulos GK, DeFrances MC. Liver regeneration. Science 1997;276:60–66. [PubMed: 9082986]
5. Higgins GM, Anderson RM. Experimental pathology of liver: Restoration of liver of the white rat following partial surgical removal. Arch. Pathol 1931;12:186–202.
6. Michalopoulos GK. Liver regeneration after partial hepatectomy: critical analysis of mechanistic dilemmas. Am J Pathol 2010;176:2–13. [PubMed: 20019184]
7. Taub R Liver regeneration: from myth to mechanism. Nat Rev Mol Cell Biol 2004;5:836–847. [PubMed: 15459664]
8. Michalopoulos GK. Hepatostat: Liver regeneration and normal liver tissue maintenance. Hepatology 2017;65:1384–1392. [PubMed: 27997988]
9. Michalopoulos GK. Principles of liver regeneration and growth homeostasis. Compr Physiol 2013;3:485–513. [PubMed: 23720294]
10. Zhou YM, Li B, Xu DH, Yang JM. Safety and efficacy of partial hepatectomy for huge (>/=10 cm) hepatocellular carcinoma: a systematic review. Med Sci Monit 2011;17:RA76–83. [PubMed: 21358616]
11. Jeon H, Lee SG. Living donor liver transplantation. Curr Opin Organ Transplant 2010;15:283–287. [PubMed: 20489627]
12. Mehendale HM. Tissue repair: an important determinant of final outcome of toxicant-induced injury. Toxicol Pathol 2005;33:41–51. [PubMed: 15805055]
13. Bhushan B, Apte U. Liver Regeneration after Acetaminophen Hepatotoxicity: Mechanisms and Therapeutic Opportunities. Am J Pathol 2019;189:719–729. [PubMed: 30653954]
14. Mehendale HM. Role of hepatocellular regeneration and hepatolobular healing in the final outcome of liver injury. A two-stage model of toxicity. Biochem Pharmacol 1991;42:1155–1162. [PubMed: 1716097]
15. Soni MG, Mehendale HM. Role of tissue repair in toxicologic interactions among hepatotoxic organics. Environ Health Perspect 1998;106 Suppl 6:1307–1317. [PubMed: 9860886]
16. Soni MG, Ramaiah SK, Mumtaz MM, Clewell H, Mehendale HM. Toxicant-inflicted injury and stimulated tissue repair are opposing toxicodynamic forces in predictive toxicology. Regul Toxicol Pharmacol 1999;29:165–174. [PubMed: 10341147]

17. Bhushan B, Walesky C, Manley M, Gallagher T, Borude P, et al. Pro-regenerative signaling after acetaminophen-induced acute liver injury in mice identified using a novel incremental dose model. Am J Pathol 2014;184:3013–3025. [PubMed: 25193591]
18. Bhushan B, Borude P, Edwards G, Walesky C, Cleveland J, et al. Role of bile acids in liver injury and regeneration following acetaminophen overdose. Am J Pathol 2013;183:1518–1526. [PubMed: 24007882]
19. Bhushan B, Edwards G, Desai A, Michalopoulos GK, Apte U. Liver-Specific Deletion of Integrin-Linked Kinase in Mice Attenuates Hepatotoxicity and Improves Liver Regeneration After Acetaminophen Overdose. Gene Expr 2016;17:35–45. [PubMed: 27125733]
20. Bhushan B, Poudel S, Manley MW Jr., Roy N, Apte U. Inhibition of Glycogen Synthase Kinase 3 Accelerated Liver Regeneration after Acetaminophen-Induced Hepatotoxicity in Mice. Am J Pathol 2017;187:543–552. [PubMed: 28068511]
21. Apte U, Singh S, Zeng G, Cieply B, Virji MA, et al. Beta-catenin activation promotes liver regeneration after acetaminophen-induced injury. Am J Pathol 2009;175:1056–1065. [PubMed: 19679878]
22. Dalhoff K, Laursen H, Bangert K, Poulsen HE, Anderson ME, et al. Autoprotection in acetaminophen intoxication in rats: the role of liver regeneration. Pharmacol Toxicol 2001;88:135–141. [PubMed: 11245408]
23. Schmidt LE, Dalhoff K. Alpha-fetoprotein is a predictor of outcome in acetaminophen-induced liver injury. Hepatology 2005;41:26–31. [PubMed: 15690478]
24. Bhushan B, Chavan H, Borude P, Xie Y, Du K, et al. Dual Role of Epidermal Growth Factor Receptor in Liver Injury and Regeneration after Acetaminophen Overdose in Mice. Toxicol Sci 2017;155:363–378. [PubMed: 28123000]
25. Nourjah P, Ahmad SR, Karwoski C, Willy M. Estimates of acetaminophen (Paracetomal)-associated overdoses in the United States. Pharmacoepidemiol Drug Saf 2006;15:398–405. [PubMed: 16294364]
26. Lee WM. Acetaminophen-related acute liver failure in the United States. Hepatol Res 2008;38:S3–S8. [PubMed: 19125949]
27. Lee WM. Etiologies of acute liver failure. Semin Liver Dis 2008;28:142–152. [PubMed: 18452114]
28. Borude P, Edwards G, Walesky C, Li F, Ma X, et al. Hepatocyte specific deletion of farnesoid X receptor delays, but does not inhibit liver regeneration after partial hepatectomy in mice. Hepatology 2012;56:2344–2352. [PubMed: 22730081]
29. Fausto N, Campbell JS, Riehle KJ. Liver regeneration. Hepatology 2006;43:S45–53. [PubMed: 16447274]
30. Paranjpe S, Bowen WC, Mars WM, Orr A, Haynes MM, et al. Combined systemic elimination of MET and epidermal growth factor receptor signaling completely abolishes liver regeneration and leads to liver decompensation. Hepatology 2016;64:1711–1724. [PubMed: 27397846]
31. Bird TG, Muller M, Boulter L, Vincent DF, Ridgway RA, et al. TGFbeta inhibition restores a regenerative response in acute liver injury by suppressing paracrine senescence. Sci Transl Med 2018;10.
32. McMillin M, Grant S, Frampton G, Petrescu AD, Williams E, et al. The TGFbeta1 Receptor Antagonist GW788388 Reduces JNK Activation and Protects Against Acetaminophen Hepatotoxicity in Mice. Toxicol Sci 2019;170:549–561. [PubMed: 31132129]
33. Mangipudy RS, Chanda S, Mehendale HM. Hepatocellular regeneration: key to thioacetamide autoprotection. Pharmacol Toxicol 1995;77:182–188. [PubMed: 8884881]
34. Thakore KN, Mehendale HM. Role of hepatocellular regeneration in CCl4 autoprotection. Toxicol Pathol 1991;19:47–58. [PubMed: 2047707]
35. Apte U, Mehendale HM: Hepatic defenses against toxicology: liver regeneration and tissue repair In: McQueen CA, ed. Comprehensive Toxicology. 2 ed. Philadelphia: Elsevier, 2009; 339–367.
36. Tsagianni A, Mars WM, Bhushan B, Bowen WC, Orr A, et al. Combined Systemic Disruption of MET and Epidermal Growth Factor Receptor Signaling Causes Liver Failure in Normal Mice. Am J Pathol 2018;188:2223–2235. [PubMed: 30031724]

37. Bhushan B, Stoops JW, Mars WM, Orr A, Bowen WC, et al. TCPOBOP-Induced Hepatomegaly and Hepatocyte Proliferation are Attenuated by Combined Disruption of MET and EGFR Signaling. Hepatology 2019;69:1702–1718. [PubMed: 29888801]

38. James LP, Lamps LW, McCullough S, Hinson JA. Interleukin 6 and hepatocyte regeneration in acetaminophen toxicity in the mouse. Biochem Biophys Res Commun 2003;309:857–863. [PubMed: 13679052]

39. James LP, Kurten RC, Lamps LW, McCullough S, Hinson JA. Tumour necrosis factor receptor 1 and hepatocyte regeneration in acetaminophen toxicity: a kinetic study of proliferating cell nuclear antigen and cytokine expression. Basic Clin Pharmacol Toxicol 2005;97:8–14. [PubMed: 15943753]

40. Chiu H, Gardner CR, Dambach DM, Durham SK, Brittingham JA, et al. Role of tumor necrosis factor receptor 1 (p55) in hepatocyte proliferation during acetaminophen-induced toxicity in mice. Toxicol Appl Pharmacol 2003;193:218–227. [PubMed: 14644624]

41. Borude P, Bhushan B, Gunewardena S, Akakpo J, Jaeschke H, et al. Pleiotropic Role of p53 in Injury and Liver Regeneration after Acetaminophen Overdose. Am J Pathol 2018;188:1406–1418. [PubMed: 29654721]

42. Borude P, Bhushan B, Apte U. DNA Damage Response Regulates Initiation of Liver Regeneration Following Acetaminophen Overdose. Gene Expr 2018;18:115–123. [PubMed: 29540258]

43. Viswanathan P, Sharma Y, Gupta P, Gupta S. Replicative stress and alterations in cell cycle checkpoint controls following acetaminophen hepatotoxicity restrict liver regeneration. Cell Prolif 2018;51:e12445. [PubMed: 29504225]

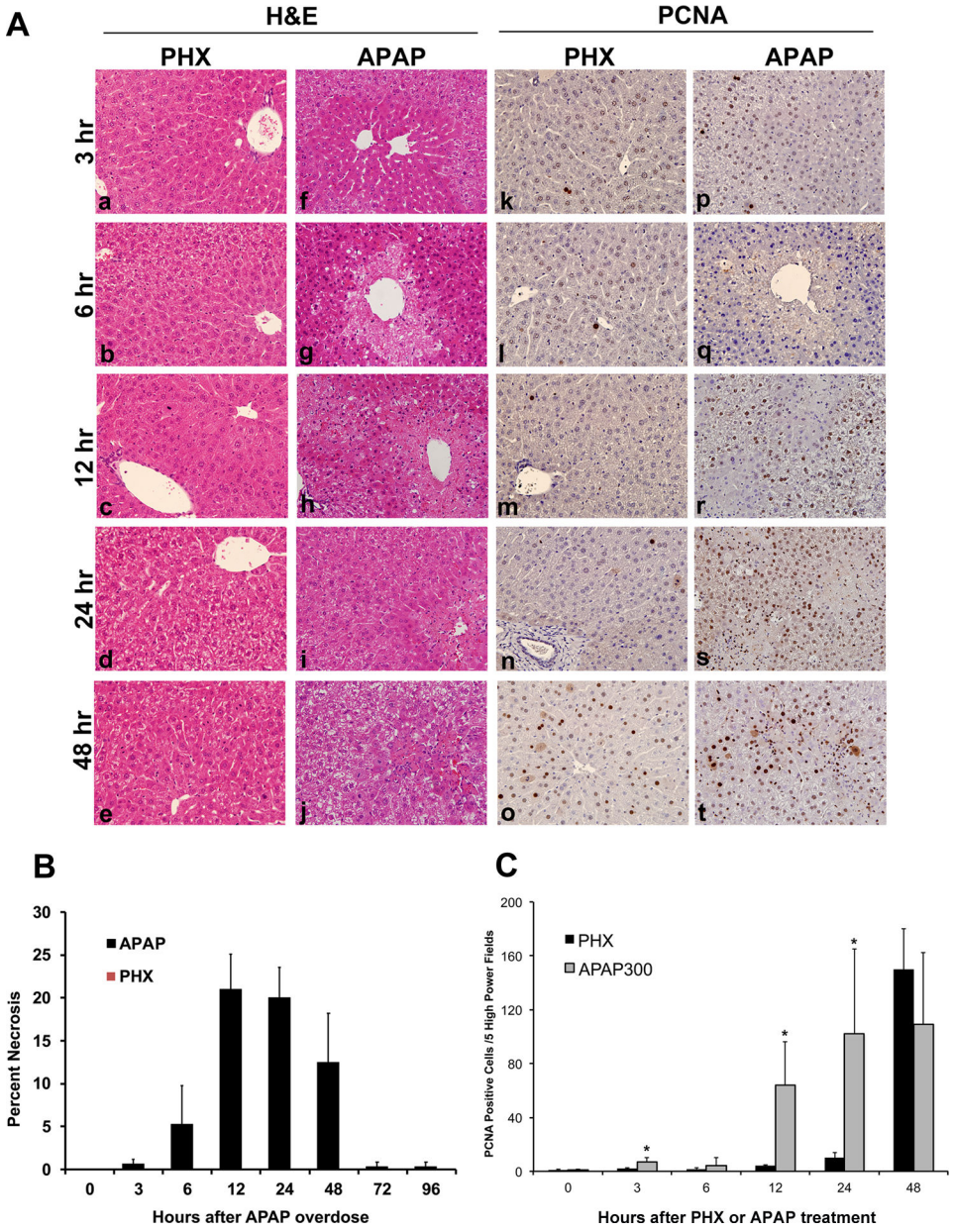

Figure 1. Differences in histopathological changes and kinetics of cell proliferation during liver regeneration after PHX and regeneration after APAP-induced ALF.

Representative photomicrographs of H&E stained liver sections after PHX (a to e) and APAP treatment (f to j). Representative photomicrographs of PCNA immunohistochemical staining on liver sections of mice subjected to PHX (k to o) and those treated with APAP (p to t). All images are at 400x magnification. (u) Bar graph showing counts of PCNA positive cells in APAP and PHX groups at various time points.

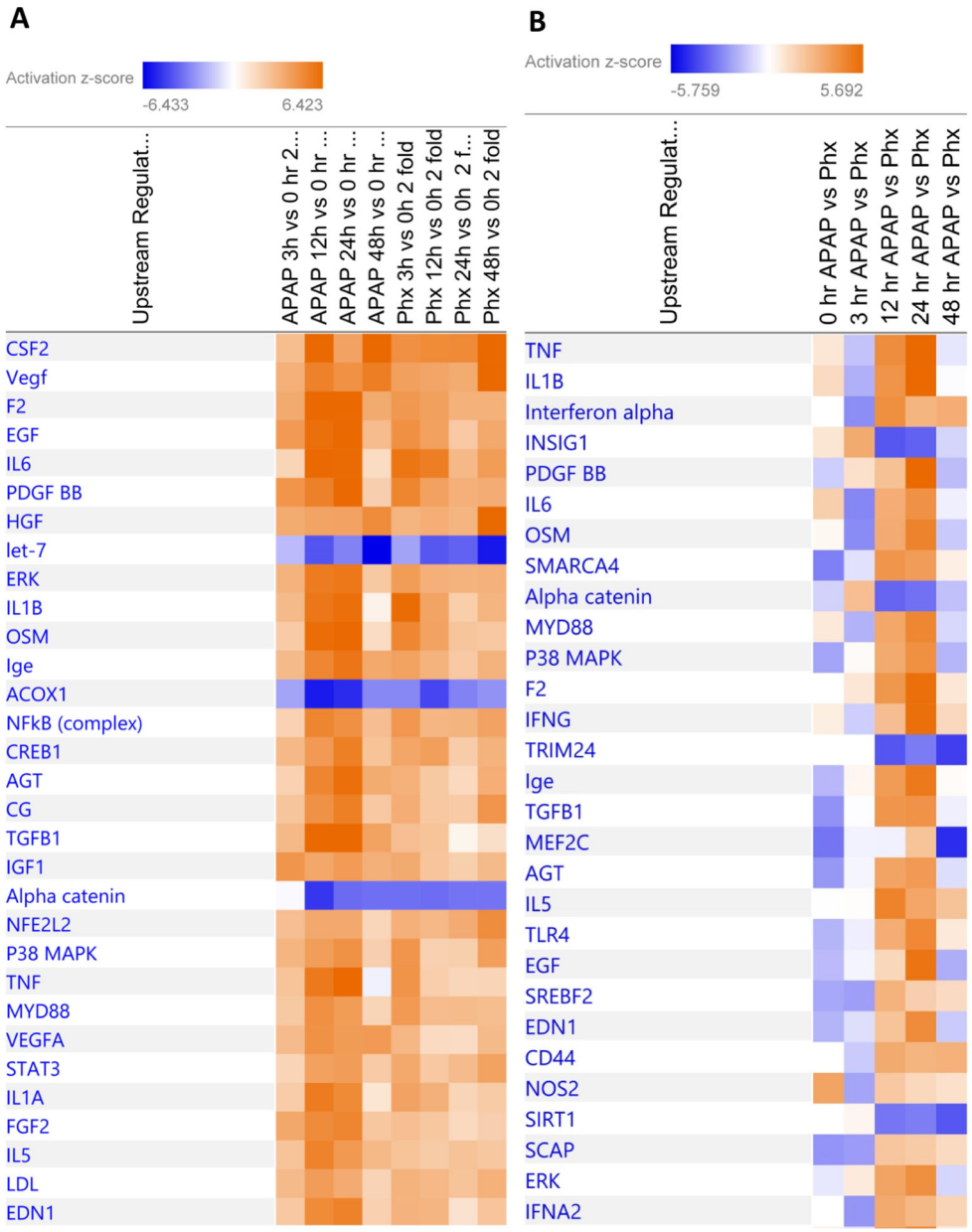

Figure 2.

(A) Heat-map showing comparison of top 30 upstream regulators predicted to be alerted at various time points after APAP300 or PHX compared to basal levels as analyzed using Ingenuity Pathway Analysis (IPA). Genes which were upregulated or downregulated at least 2 fold at various time points (3, 12, 24 and 48 hr) vs 0 hr in APAP300 or PHX group were used for analysis. **(B) Heat-map showing comparison of top 30 upstream regulators predicted to be alerted in APAP300 vs PHX group at various time points as analyzed using Ingenuity Pathway Analysis (IPA).** Genes which were upregulated or downregulated at least 2 fold in APAP300 vs PHX group at various time points (0, 3, 12, 24 and 48 hr) were used for analysis. Upstream regulators were predicted based on analysis of downstream gene network taking directionality and fold change of each

gene into consideration. (Orange: predicted activation; Blue: predicted inhibition; intensity of color reflect z-score value for activation/inhibition)

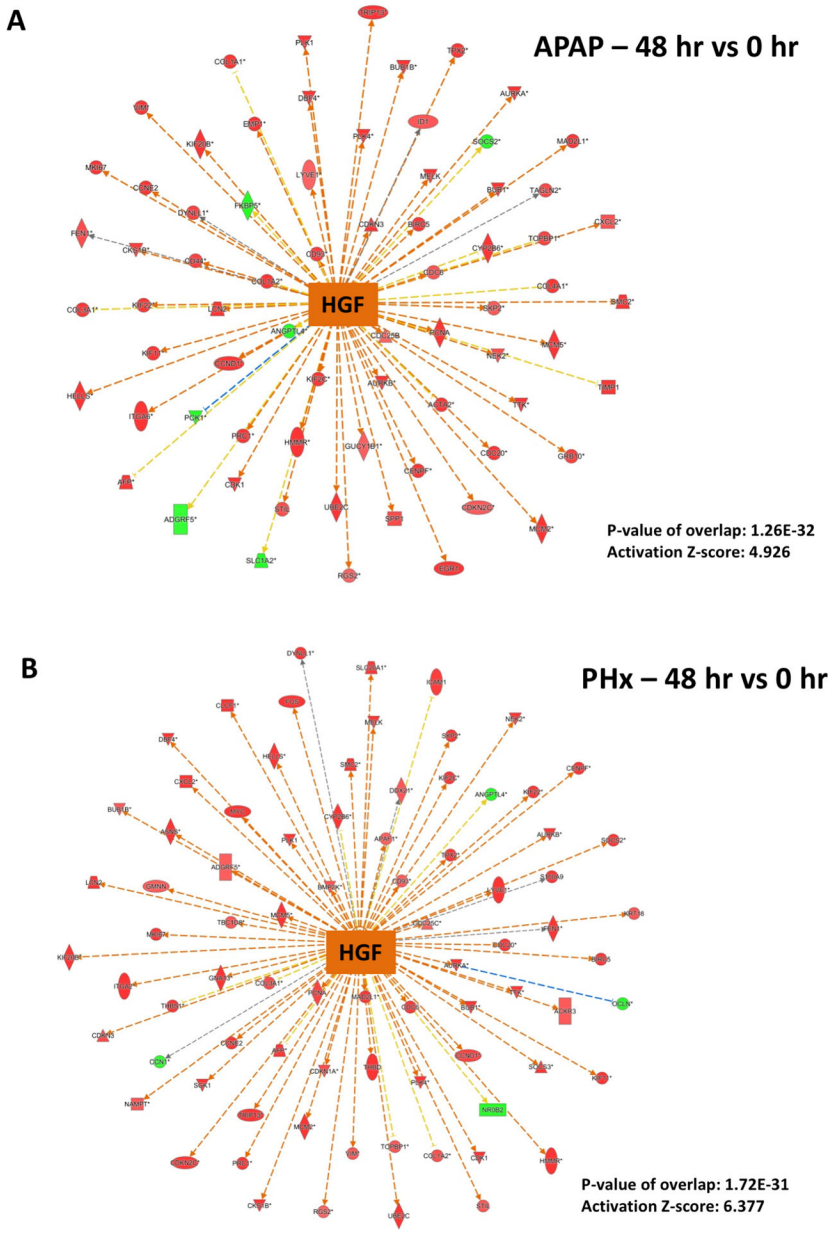

Figure 3. Predicted activation of HGF signaling after both APAP300 and PHX.

Ingenuity Pathway Analysis (IPA) of microarray data showing predicted activation of HGF signaling at 48 hr (vs 0 hr) after (A) APAP 300 and (B) PHX, based on downstream gene expression profile. Positive z-score (absolute z-score > 2 considered as significant) represents predicted activation of upstream regulator based on expression profile of downstream genes. p-values signifies extent of overlap between set of downstream target genes of a upstream regulator in dataset compared to all known downstream target genes of that upstream regulator in the reference genome. (red shapes: upregulated genes; green shapes: downregulated genes with intensity of color reflecting extent of upregulation or downregulation; orange center shape: predicted activation)

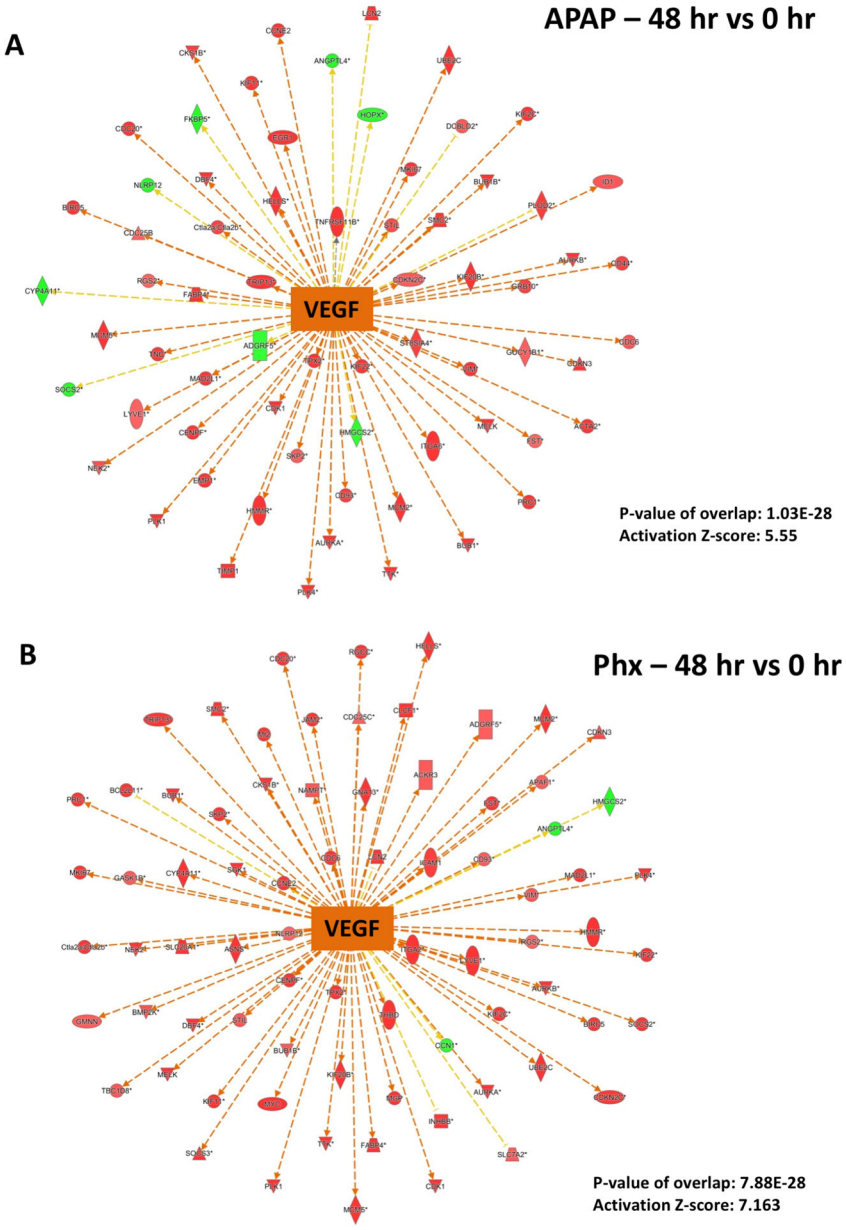

Figure 4. Predicted activation of VEGF signaling after both APAP300 and PHX.

Ingenuity Pathway Analysis (IPA) of microarray data showing predicted activation of VEGF signaling at 48 hr (vs 0 hr) after (A) APAP 300 and (B) PHX, based on downstream gene expression profile. Positive z-score (absolute z-score > 2 considered as significant) represents predicted activation of upstream regulator based on expression profile of downstream genes. p-values signifies extent of overlap between set of downstream target genes of a upstream regulator in dataset compared to all known downstream target genes of that upstream regulator in the reference genome. (red shapes: upregulated genes; green shapes: downregulated genes with intensity of color reflecting extent of upregulation or downregulation; orange center shape: predicted activation)

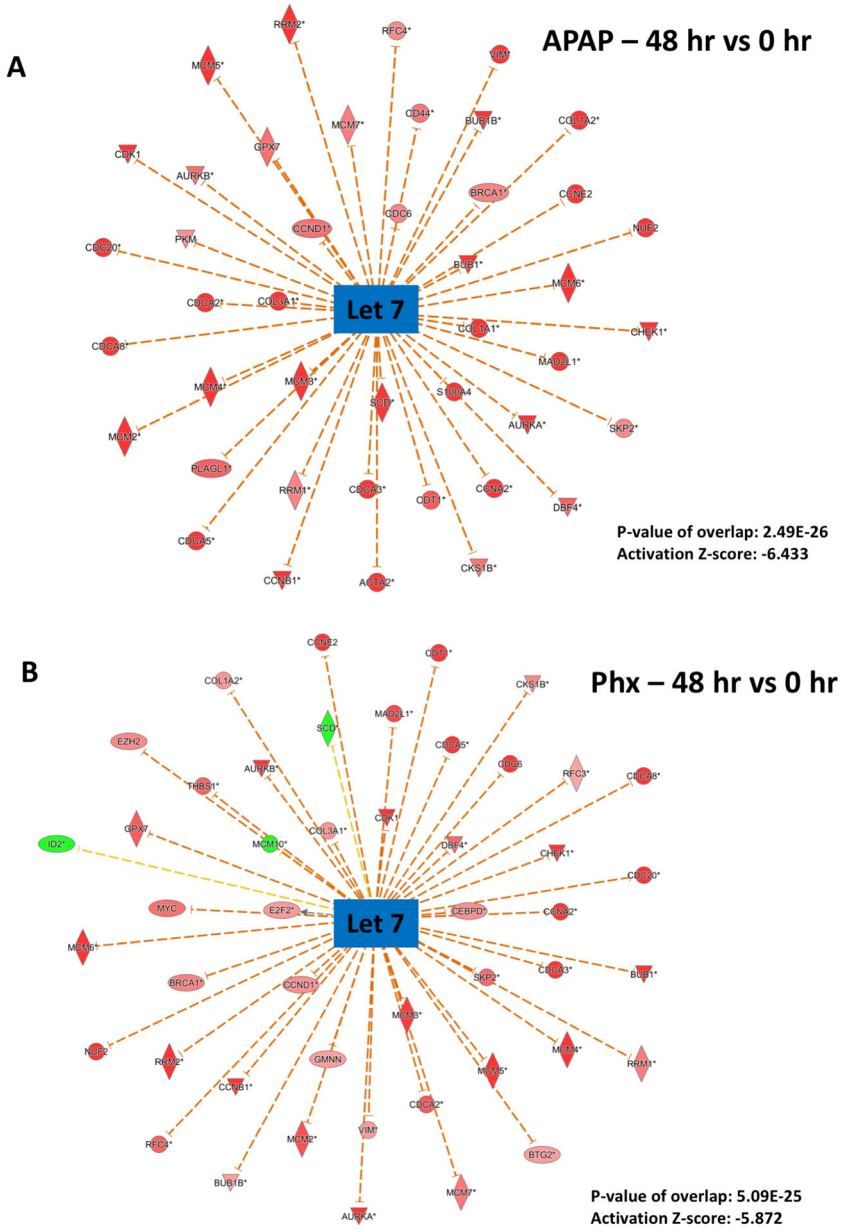

Figure 5. Predicted inhibition of Let-7 miRNA after both APAP300 and PHX.

Ingenuity Pathway Analysis (IPA) of microarray data showing predicted inhibition of Let-7 at 48 hr (vs 0 hr) after (A) APAP 300 and (B) PHX, based on downstream gene expression profile. Most of the downstream genes which are known to be inhibited by Let 7 miRNA are induced after both APAP and Phx. Negative z-score (absolute z-score > 2 considered as significant) represents predicted inhibition of upstream regulator based on expression profile of downstream genes. p-values signifies extent of overlap between set of downstream target genes of a upstream regulator in dataset compared to all known downstream target genes of that upstream regulator in the reference genome. (red shapes: upregulated genes; green shapes: downregulated genes with intensity of color reflecting extent of upregulation or downregulation; blue center shape: predicted inhibition)

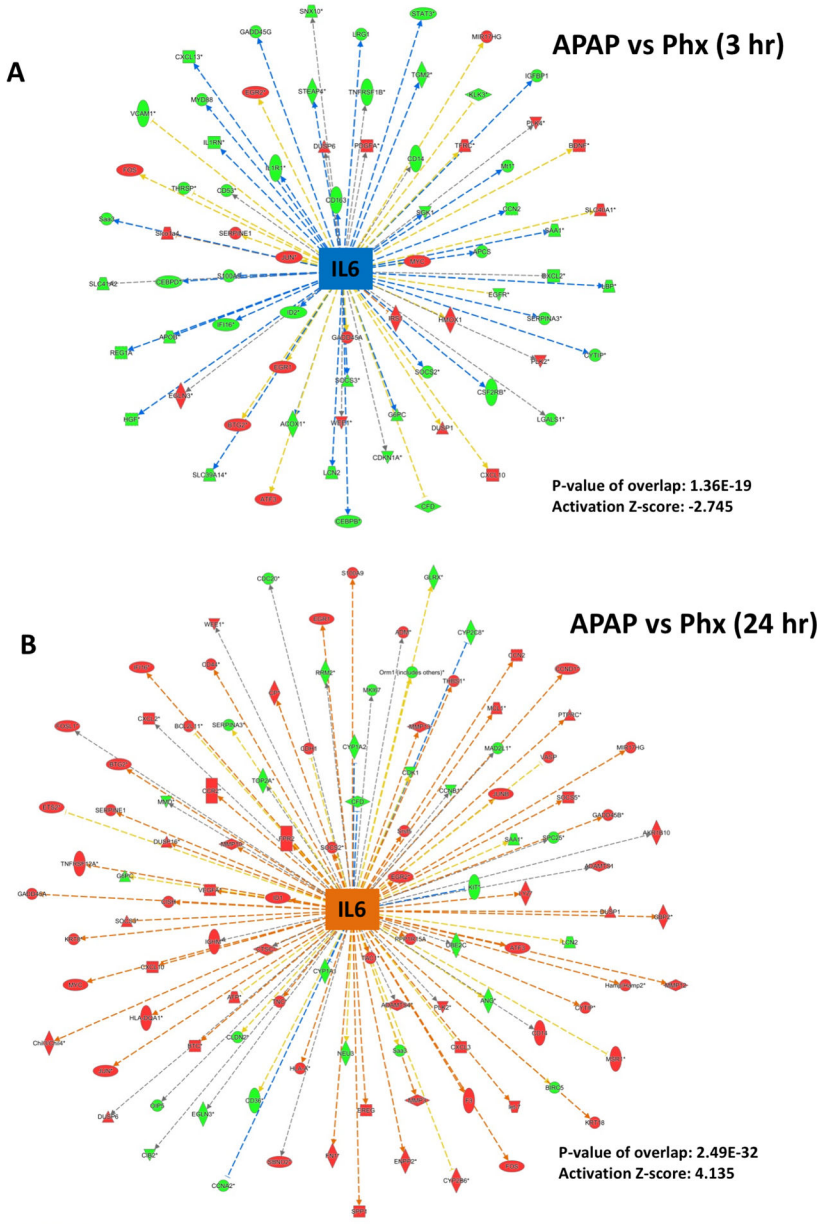

Figure 6. Temporal differences in activation of IL6 signaling after APAP300 and PHX.

Ingenuity Pathway Analysis (IPA) of microarray data showing (A) predicted inhibition of IL6 signaling at 3 hr and (B) activation at 24 hr after APAP 300 compared to PHX, based on downstream gene expression profile. As shown in Figure 2, IL6 was activated as early as 3 hr after PHX, while activation was delayed (starting from 12 hr) after APAP300. Positive or negative z-score (absolute z-score > 2 considered as significant) represents predicted activation or inhibition of upstream regulator based on expression profile of downstream genes. p-values signifies extent of overlap between set of downstream target genes of a upstream regulator in dataset compared to all known downstream target genes of that upstream regulator in the reference genome. (red shapes: upregulated genes; green shapes: downregulated genes with intensity of color reflecting extent of upregulation or

downregulation; blue center shape: predicted inhibition; orange center shape: predicted activation)

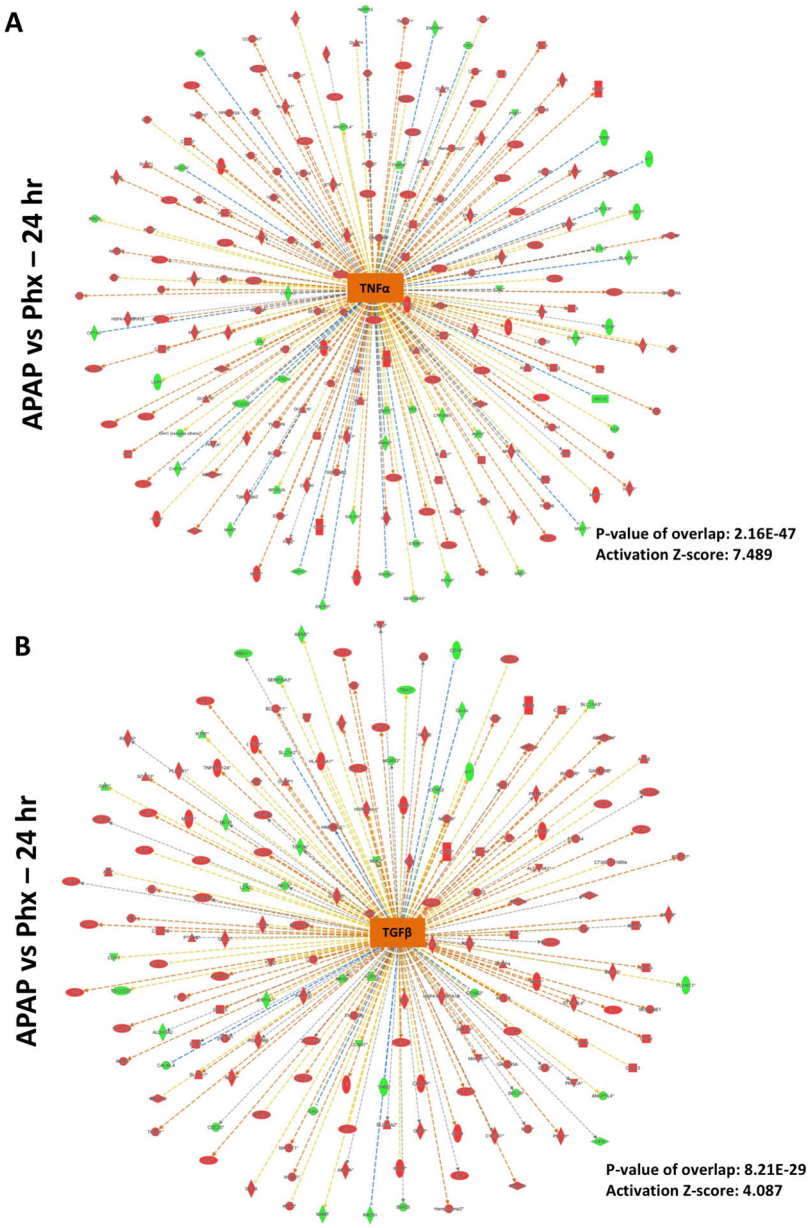

Figure 7. Predicted activation of TNFα and TGFβ signaling after APAP300 compared to PHX at 24 hr.

Ingenuity Pathway Analysis (IPA) of microarray data showing predicted activation of (A) TNFα signaling and (B) TGFβ signaling at 24 hr in APAP 300 group vs PHX, based on downstream gene expression profile. Positive z-score (absolute z-score > 2 considered as significant) represents predicted activation of upstream regulator based on expression profile of downstream genes. p-values signifies extent of overlap between set of downstream target genes of a upstream regulator in dataset compared to all known downstream target genes of that upstream regulator in the reference genome. (red shapes: upregulated genes; green shapes: downregulated genes with intensity of color reflecting extent of upregulation or downregulation; orange center shape: predicted activation)

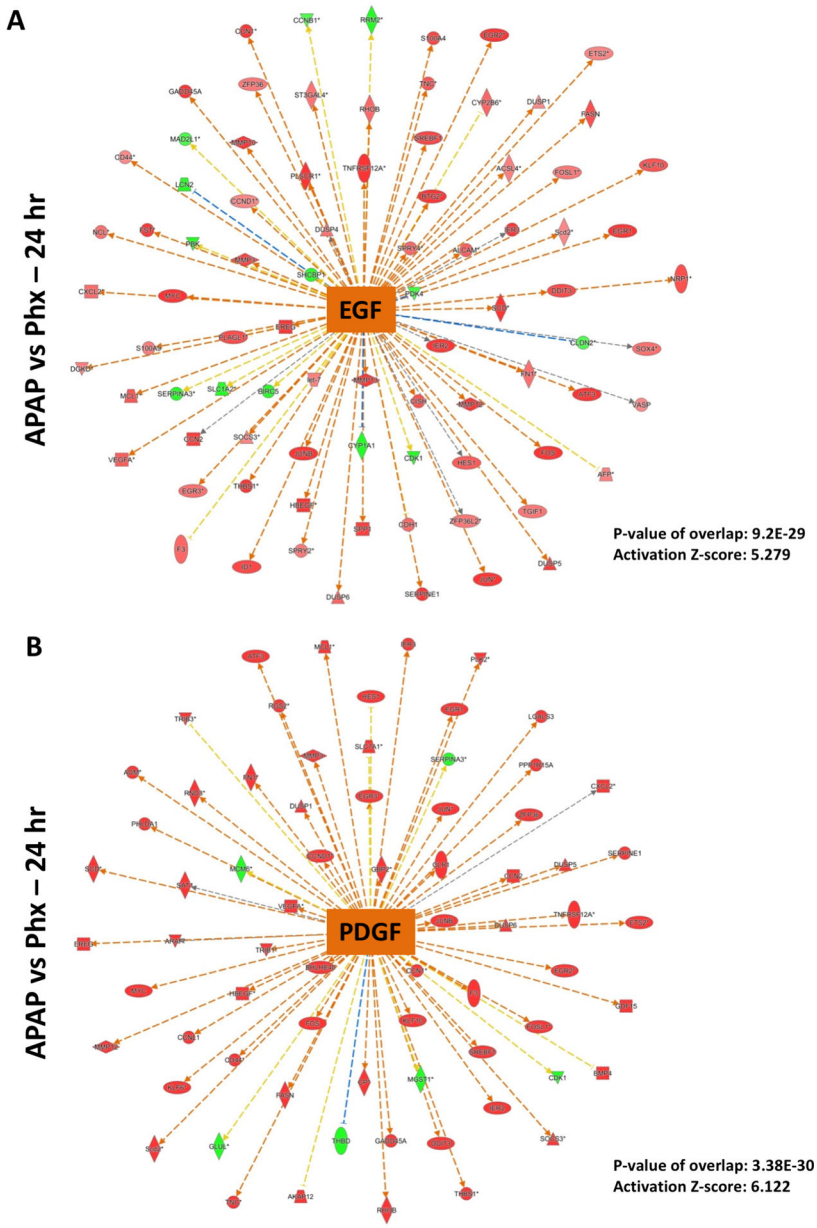

Figure 8. Predicted activation of EGF and PDGF signaling after APAP300 compared to PHX at 24 hr.

Ingenuity Pathway Analysis (IPA) of microarray data showing predicted activation of (A) EGF signaling and (B) PDGF signaling at 24 hr in APAP 300 group vs PHX, based on downstream gene expression profile. Positive z-score (absolute z-score > 2 considered as significant) represents predicted activation of upstream regulator based on expression profile of downstream genes. p-values signifies extent of overlap between set of downstream target genes of a upstream regulator in dataset compared to all known downstream target genes of that upstream regulator in the reference genome. (red shapes: upregulated genes; green shapes: downregulated genes with intensity of color reflecting extent of upregulation or downregulation; orange center shape: predicted activation)

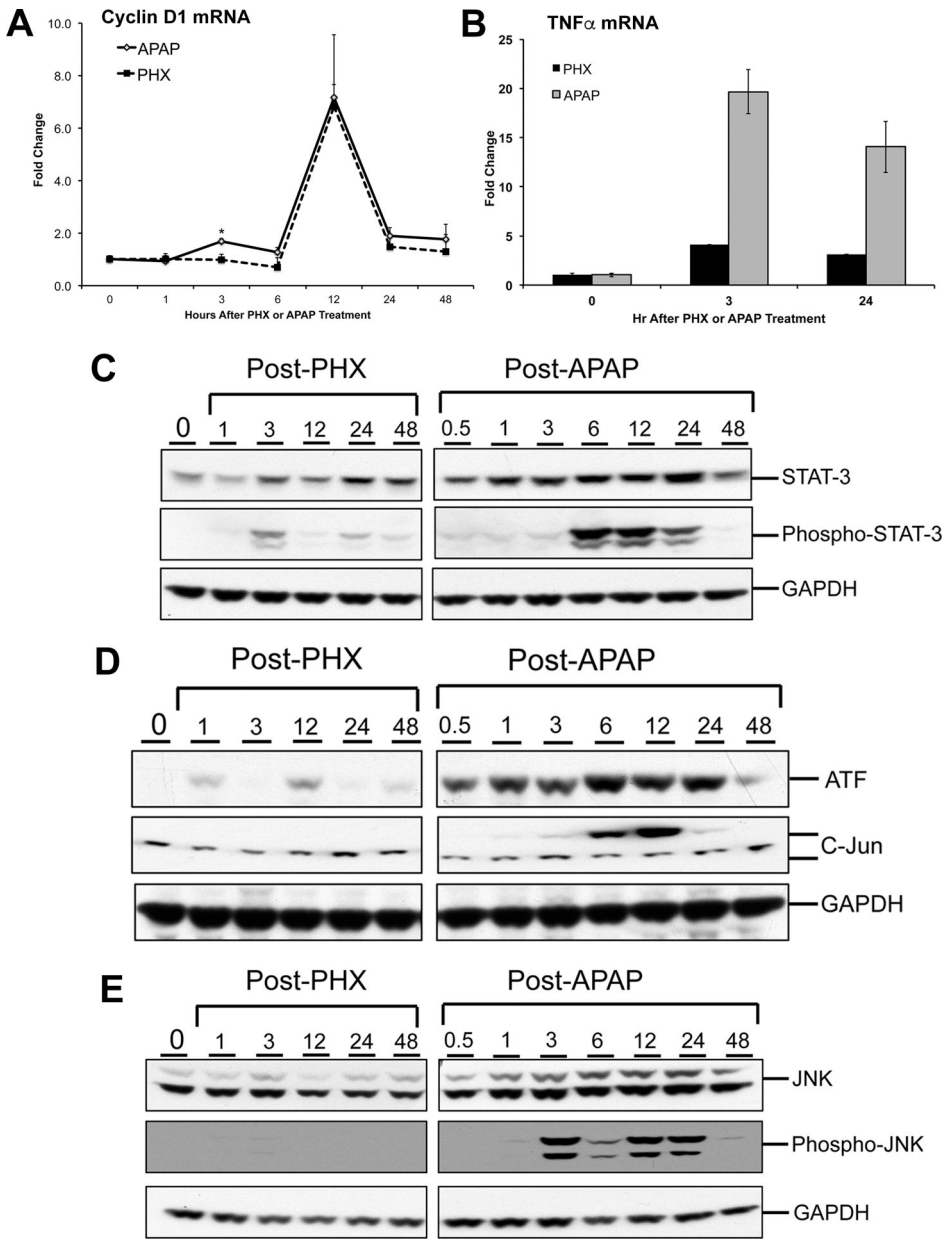

Figure 9. Conformation of selected microarray findings.

mRNA expression of (A) Cyclin D1, (B) TNF-α and Western blot analysis of (C) STAT-3, phospho-STAT3, (D) ATF, c-JUN and (E) JNK1/2 and phosho-JNK 1/2 at various time points after APAP overdose (300 mg/kg) or partial hepatectomy (PHX) in mice.

Table 1.

Differences in PHX and DILI models relevant to liver regeneration

Parameter	Partial Hepatectomy	DILI
Point of initiation	Well defined, within minutes after surgery	Not well defined, depends on cellular damage
Role of Inflammation	Minor inflammatory response	Significant inflammatory response
Cell cycle progression	Synchronized	Unsynchronized (depends on extent of cell death)
Cell proliferation	All hepatocytes in the remnant liver divide	Hepatocytes surrounding the necrotic zone divide